J. Electroanal. Chem., 163 (1984) 371–379
Elsevier Sequoia S.A., Lausanne – Printed in The Netherlands

Short communication

REDOX THERMODYNAMICS OF SURFACE-BOUND REACTANTS

ILLUSTRATIVE BEHAVIOR OF COBALT(III)/(II) MACROBICYCLIC "CAGE" COMPLEXES

J.T. HUPP and H.Y. LIU

Department of Chemistry, Purdue University, West Lafayette, IN 47907 (U.S.A.)

P.A. LAY, W.H.F. PETRI and A.M. SARGESON

Research School of Chemistry, Australian National University, Canberra ACT 2600 (Australia)

M.J. WEAVER *

Department of Chemistry, Purdue University, West Lafayette, IN 47907 (U.S.A.)

(Received 2nd June 1983; in revised form 12th September 1983)

The electrochemistry of surface-bound redox couples is an area of considerable current interest [1]. In addition to their potential applications in electrocatalysis, such couples that involve mechanistically uncomplicated one-electron transfer offer opportunities for studying several fundamental aspects of heterogeneous electron-transfer processes. For example, the interpretation of electrochemical rate parameters for surface-attached reactants is especially straightforward, since these provide direct information on the energetics of the elementary electron-transfer step [2].

The comparison between redox thermodynamics of a given redox couple in solution and in the surface-bound state are expected to yield useful insights into the differences in the solvating environment between the interfacial region and the bulk solution. Bulk solution and surface thermodynamic behavior for two Co(III)/(II) redox couples adsorbed by different means is presented here in order to illustrate the virtues of such analyses for simple electrode reactions. The structures of these two macrobicyclic ("sarcophagene") couples [3], Co(EFMEoxosar-H)$^{2+/+}$ and Co(diNOsar)$^{3+/2+}$ **, are shown in Figs. 1a and 1b, respectively. These complexes are extremely stable in both oxidation states, yielding chemically reversible one-electron transfer in a variety of solvents [4]. The cobalt salts Co(EFMEoxosar-H)$(CF_3SO_3)_2$ and Co(diNOsar)$(ClO_4)_3$ used here were prepared as described in ref. 5.

The Co(EFMEoxosar-H)$^{2+/+}$ couple was found to be strongly adsorbed at mercury, both from water and N-methylformamide (NMF). Cyclic voltammetric

* To whom correspondence should be addressed.

** [Co(EFMEoxosar-H)]$^{2+}$ = [1-carboxyethyl-8-methyl-2-oxo-3,6,10,13,16,19-hexaazabicylo[6.6.6]-icosanato(1 –)]cobalt(III); [Co(diNOsar)]$^{3+}$ = (1,8-dinitro-3,6,10,13,16,19-hexaazabicyclo[6.6.6]-icosane)cobalt(III).

0022-0728/84/$03.00

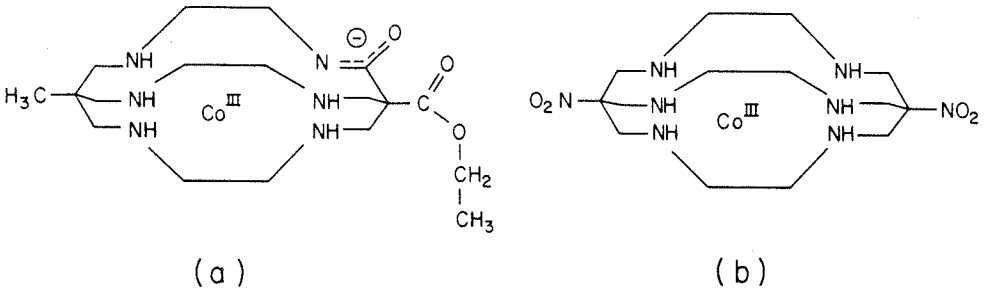

Fig. 1. (a) Structure of Co(EFMEoxosar-H)$^{2+}$. (b) Structure of Co(diNOsar)$^{3+}$.

waves due almost entirely to reaction of adsorbed material were obtained by using dilute solutions of the Co(III) complex (30–100 μM) together with rapid scan rates (10–200 V s^{-1}). Measurements were made at a hanging mercury drop electrode with either 0.1 M KPF_6 or 1 M $NaClO_4$ as supporting electrolyte. The electrochemical measurements utilized a PAR 173 potentiostat with a PAR 175 potential programmer, the voltammetric traces being recorded using a Nicolet Explorer I oscilloscope coupled to a Houston 2000 X–Y recorder. Cyclic voltammograms for the bulk

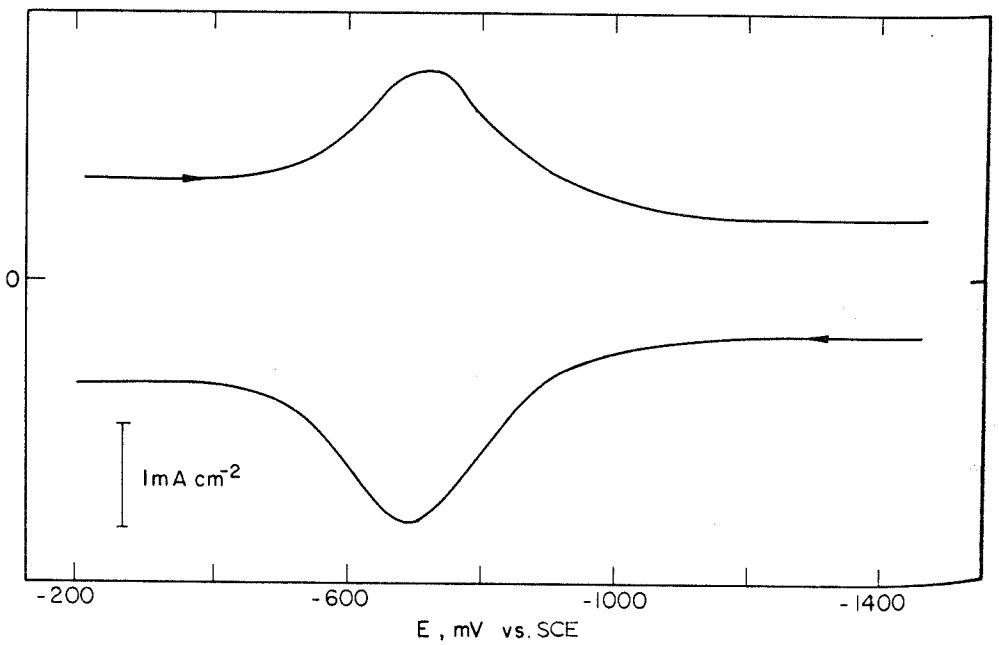

Fig. 2. Cyclic voltammogram for surface-bound Co(EFMEoxosar-H)$^{2+/+}$ at mercury in aqueous 1.0 M $NaClO_4$ at 25°C. Reactant concentration = 50 μM. Scan rate = 10 V s^{-1}.

redox couple were obtained using slower sweep rates (100–500 mV s^{-1}) and higher bulk concentrations (ca. 1 mM). Other experimental details are given elsewhere [6]

A cyclic voltammogram for the Co(EFMEoxosar-H)$^{2+/+}$ surface-bound couple in a 0.1 M aqueous KPF_6 is shown in Fig. 2. The symmetrical shape of the voltammogram and the identical peak potentials for the anodic and cathodic waves are indicative of a reversible surface process, while the 230 mV peak width at half height can be interpreted as evidence of repulsive interactions between the adsorbed cations [7]. Reversible behavior persists at least to scan rates of 200 V s^{-1}. Thus, a lower limit of ca. 5×10^3 s^{-1} is thereby indicated for the standard rate constant, k_{et}^s, of the surface-bound couple [8]. Adsorption of Co(EFMEoxosar-H)$^{2+/+}$ is perhaps a surprising finding. Given the structure of the complex it seems feasible that specific adsorption occurs through chelation at the mercury surface by the enolate and ester carbonyl groups (Fig. 1a). Although somewhat speculative, this mode of surface coordination is supported by the isolation of a binuclear complex where these carbonyl groups are coordinated to $Co(en)_2^{3+}$ (en = ethylenediamine) [9].

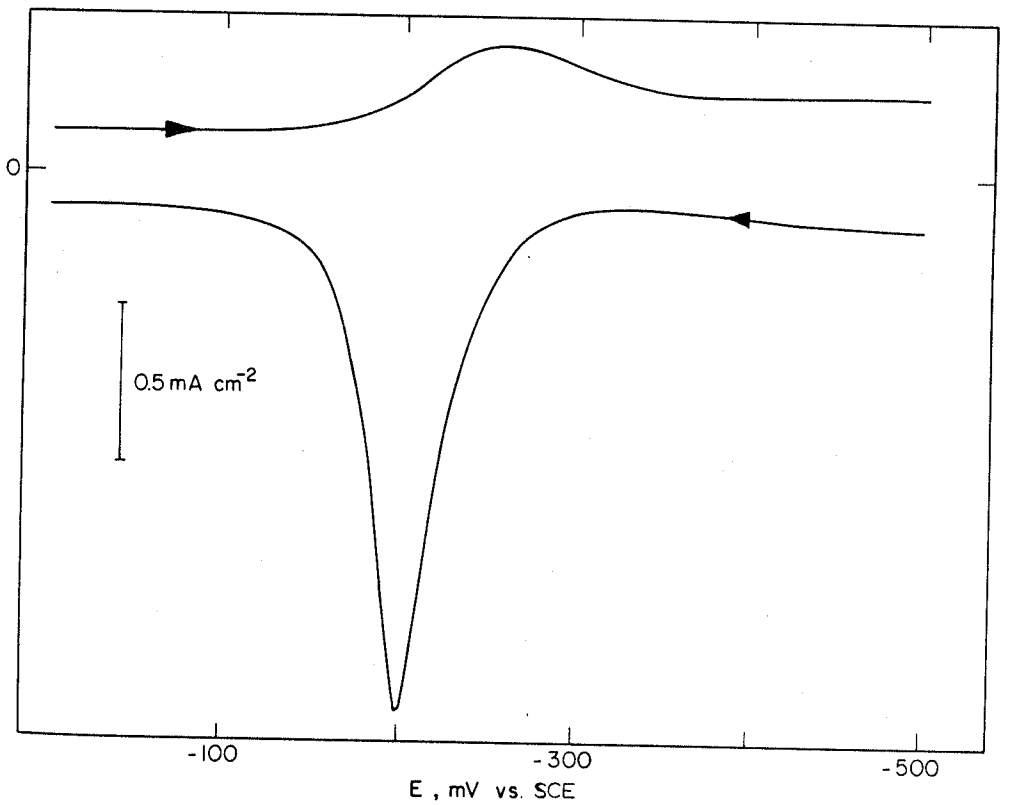

Fig. 3. Cyclic voltammogram of precipitated Co(diNOsar)$^{3+/2+}$ at mercury in aqueous 1.0 M $NaClO_4$ at 25°C. Reactant concentration = 50 μM. Scan rate = 20 V s^{-1}.

A striking contrast to the simple behavior of Co(EFMEoxosar-H)$^{2+/+}$ is found for adsorbed Co(diNOsar)$^{3+/2+}$. Cyclic voltammograms (as in Fig. 3) for the surface redox reaction of this complex in aqueous 1.0 *M* $NaClO_4$ are markedly asymmetric, exhibiting a very sharp oxidation peak and a broad reduction peak. The peak separation at a scan rate of 10 V s^{-1} is 60 mV while the anodic and cathodic peak widths at half height are 41 mV and 98 mV, respectively. The peak separation is substantially less than 60 mV at lower scan rates. A shift of the sharp anodic peak to more negative potentials occurs as the sweep rate is decreased, while the cathodic peak remains largely unaffected. The area under the reverse (cathodic) peak was generally smaller than beneath the forward (anodic) peak, especially at low sweep rates. This appears to be due to partial desorption of the more soluble Co(III) form. Stronger adsorption of the Co(II) form was also indicated from single-step chronocoulometric measurements. For both Co(EFMEoxosar-H)$^{2+/+}$ and Co(diNOsar)$^{3+/2+}$, the peak currents vary approximately linearly with scan rate, confirming that the waves arise from surface-bound rather than bulk-phase reactant.

Adsorption of Co(diNOsar)$^{3+/2+}$ is readily detected in aqueous $NaClO_4$, NaCl, and Na_2SO_4 electrolytes but is not observed in KPF_6 media. Similar behavior is seen with Co(sepulchrate)$^{3+/2+}$ * [3] and Co(en)$_3^{3+/2+}$. All three of these couples lack ligands which would normally be expected to induce specific adsorption via surface coordination. Evidently adsorption occurs instead via "surface precipitation" [10]. Thus, the solubility product of Co(diNOsar)$^{3+} \cdot X_3^-$, where X^- is the supporting electrolyte anion, can be exceeded at the mercury surface even when the complex remains soluble in the bulk solution since, as a consequence of anion specific adsorption, the concentration of ClO_4^-, Cl^- or SO_4^{2-} ions will be enhanced at the electrode surface. In addition, the diffuse-layer concentration of the positively charged complex will be increased relative to its bulk value if super-equivalent adsorption of anions occurs. The absence of specific adsorption of Co(diNOsar)$^{3+/2+}$ in KPF_6 solutions provides strong support to this explanation. Thus although the bulk solubility of the hexafluorophosphate and perchlorate salts of Co(diNOsar)$^{3+}$ are similar, PF_6^- is adsorbed only to a small extent at the mercury–aqueous solution interface in comparison to most other anions [11].

The cyclic voltammogram in Fig. 3 closely resembles those obtained by Daum and Murray [12] for ferrocene polymer film electrodes. Laviron and Roullier showed that such highly asymmetric voltammograms can be obtained when charge transfer is kinetically controlled and the composite Frumkin isotherm parameters characterizing ox–ox, red–red, ox–red and transition state–ox and –red interactions have widely differing values [13]. Their treatment can at least formally be applied to the present case. Thus, despite the obvious chemical differences, the peculiarities of surface redox reactions of poly-(vinyl ferrocene) and of adsorbed Co(diNOsar)$^{3+/2+}$ may have a common explanation.

* Sepulchrate = 1,3,5,8,10,13,16,19-octaazabicyclo[6.6.6]icosane.

Although quantitative determinations of k_{et}^{s} are precluded, the quasi-reversible behavior of adsorbed Co(diNosar)$^{3+/2+}$ indicates that this couple exhibits substantially smaller values of k_{et}^{s} than adsorbed Co(EFMEoxosar-H)$^{2+/+}$ even though the outer-sphere redox reactivities of these two couples are similar [5]. The abnormally sluggish kinetics for the former system may arise from structural changes in the adsorbed layer, such as anion migration, associated with electron transfer. This behavior is consistent with the present interpretation of the adsorbate as a surface precipitate since it would be expected to form a structurally ordered "ionic lattice", whose two-dimensional structure may well differ in the oxidized and reduced forms. As a caveat to other experimentalists, we note that the presence of such surface precipitation can substantially influence the values of apparent heterogeneous rate parameters for the solution reactant. Surprisingly small standard rate constants ($\lesssim 5 \times 10^{-3}$ cm s^{-1}) were often obtained for Co(diNOsar)$^{2+/+}$ and other Co(III)/(II) couples under conditions where surface precipitation was encountered [4a], much faster rates generally being obtained in 0.1 M KPF_6 where surface precipitation is absent. These slow rates may be due either to unfavorable double-layer effects arising from the surface precipitate or to the presence of a reaction pathway involving surface precipitation prior to electron transfer. Ac polarography was found to be a sensitive method for detecting these complications, since waves due to the reaction of both adsorbed and bulk complexes are typically observed [4].

In addition to comparing formal potentials for corresponding surface-bound and bulk-phase couples, E_a^f and E^f respectively, it is instructive to compare their entropic components determined from the temperature coefficients of E_a^f and E^f. We have demonstrated that the difference in absolute ionic entropies, $\bar{S}^\circ_{red} - \bar{S}^\circ_{ox}$, between the reduced and oxidized forms of the bulk-phase redox couple (the so-called "reaction entropy" ΔS°_{rc}), can be obtained directly from the temperature dependence of E^f using a nonisothermal cell arrangement [6]. Reaction entropies provide a sensitive monitor of the changes in solvent polarization ("ordering") resulting from electron transfer [6,14–16]. Measurements of ΔS°_{rc} for surface-bound (or adsorbed) couples, $\Delta S^\circ_{rc,s}$, can provide similarly valuable information on the solvation changes induced by electron transfer within the interfacial environment [16].

Table 1 summarizes bulk-phase and surface thermodynamic parameters for Co(EFMEoxosar-H)$^{2+/2}$ in water and NMF. The values of E^f and E_a^f were both approximated by the mean of the cathodic- and anodic-going peak potentials, and ΔS°_{rc} and $\Delta S^\circ_{rc,s}$ determined from the temperature dependence of E^f and E_a^f, respectively, with the reference electrode held at room temperature as described in ref. 6. The reaction entropy of adsorbed Co(diNOsar)$^{3+/2+}$ is not reported, since the required values of E_a^f could not be determined with sufficient accuracy.

One interesting result is the smaller values of ΔS°_{rc} found for the surface reactions compared to the solution couples. For solution redox reactions a correlation has been found between the magnitude of ΔS°_{rc} and the degree of "internal order" of the solvent, the smallest values being found in highly structured solvents such as water [6b,15,16]. A plausible interpretation of the decreases in ΔS°_{rc} accompanying adsorption is that the redox couple experiences a relatively "more structured" solvent

TABLE 1

Comparison of thermodynamics of Co(EFMEoxosar-H)$^{2+/+}$ and Co(diNOsar)$^{3+/2+}$ in bulk solution and surface-bound environments

Couple [a]	Environment [b]	E^f/ mV vs. Fc^+/Fc [c]	ΔS°_{rc}/ J K^{-1} mol^{-1} [d]	$\Delta(\Delta G^\circ_{rc})_{s-b}$/ kJ mol^{-1} [e]	$T\Delta(\Delta S^\circ_{rc})_{s-b}$/ kJ mol^{-1} [f]	$\Delta(\Delta H^\circ_{rc})_{s-b}$/ kJ mol^{-1} [g]
Co(EFMEoxosar-H)$^{2+/+}$	surface–H_2O	−824 [h,i]	21 ± 5	−11.5	−2.5	−14.0
Co(EFMEoxosar-H)$^{2+/+}$	bulk–H_2O	−942 [h]	29 ± 4			
Co(EFMEoxosar-H)$^{2+/+}$	surface–NMF	−1227 [h]	67 ± 5	2.0	−7.5	−5.5
Co(EFMEoxosar-H)$^{2+/+}$	bulk–NMF	−1206 [h]	92 ± 4			
Co(diNOsar)$^{3+/2+}$	surface–H_2O	~ −370 [i,j]	—	−0.9	—	—
Co(diNOsar)$^{3+/2+}$	bulk–H_2O	−379 [i]	105 ± 4			

[a] For structures of redox couples, see Fig. 1.

[b] Surface was mercury in each case.

[c] Formal potential for bulk or surface-bound redox couple versus ferricinium–ferrocene couple in same solvent; determined by cyclic voltammetry as described in text. Usually reproducible to ±2 mV.

[d] Reaction entropy for bulk or surface-bound couple, as determined from $\Delta S^\circ_{rc} = F(dE^f_{ni}/dT)$, where E^f_{ni} is the formal potential measured using a nonisothermal cell arrangement (See ref. 6 for details).

[e] Free energy of transfer of redox couple from bulk to surface-bound environment, determined from $\Delta(\Delta G^\circ_{rc})_{s-b} = -F(E^f_a - E^f)$, where E^f_a and E^f are formal potentials in surface and bulk environments.

[f] Entropic component of $\Delta(\Delta G^\circ_{rc})_{s-b}$, determined from $T\Delta(\Delta S^\circ_{rc})_{s-b} = T(\Delta S^\circ_{rc,s} - \Delta S^\circ_{rc})$, where $\Delta S^\circ_{rc,s}$ and ΔS°_{rc} are reaction entropies of surface-bound and bulk redox couples, respectively.

[g] Enthalpic component of $\Delta(\Delta G^\circ_{rc})_{s-b}$, determined from $\Delta(\Delta H^\circ_{rc})_{s-b} = \Delta(\Delta G^\circ_{rc})_{s-b} + T\Delta(\Delta S^\circ_{rc})_{s-b}$.

[h] Determined in 0.1 *M* KPF_6.

[i] Determined in 1 *M* $NaClO_4$.

[j] Estimated by extrapolating measured $E_{1/2}$ to zero voltammetric sweep rate.

environment at the surface than in solution. This increased structuring could be induced by orientation of the solvent at the mercury surface. It seems likely that solvent molecules thus constrained would be less able than their bulk solution counterparts to undergo the charge-induced reorientations that largely determine reaction entropies [6]. However, only small differences in ΔS°_{rc} have been observed between related surface-bound and bulk-solution ferrocene couples, where the redox center lies within the diffuse layer [16]. An alternative, and more likely, additional explanation of the decreases in ΔS°_{rc} attending reactant adsorption is that the surface-bound couple is partially desolvated within the inner layer and therefore polarizes fewer solvent molecules than it would in bulk solution. In any case, it is evident that Co(EFMEoxosar-H)$^{2+/+}$ experiences a significantly different solvent environment at the electrode than in solution.

Significant differences between E^f and E^f_a are also found. These are expressed in terms of differences in reaction free energy [6b], $\Delta(\Delta G^\circ_{rc})_{s-b}$, between the surface and bulk redox couples, where $\Delta(\Delta G^\circ_{rc})_{s-b} = -F(E^f_a - E^f)$. The corresponding entropic and enthalpic components, $\Delta(\Delta S^\circ_{rc})_{s-b}$ and $\Delta(\Delta H^\circ_{rc})_{s-b}$, are also listed in Table 1. An interesting finding is that both enthalpic and entropic factors, acting in opposing directions, are important in determining the changes in redox potential attending adsorption.

Further insights into the factors influencing reactant solvation at electrode surfaces as well as in bulk solution can be obtained by examining the changes in redox thermodynamics brought about by altering the solvent. Gibbs energies of transfer from water to NMF, $\Delta(\Delta G^\circ_{rc})_{NMF-H_2O}$, for Co(EFME-oxosar)$^{2+/+}$ in both bulk and interfacial environments, along with related data for some structurally related cobalt complexes, are shown in Table 2. These were calculated from the formal potentials in the two solvents on the basis of the TATB assumption as described in ref. 6b. The uniformly positive transfer free energies are consistent with the greater solvent donicity for NMF than water [17]. Thus the stronger donor–acceptor interactions between the NMF solvent and the amine hydrogens should yield negative transfer free energies for both Co(III) and Co(II) forms, but to a greater extent with the former, yielding positive values of $\Delta(\Delta G^\circ_{rc})_{NMF-H_2O}$ [6b]. It is interesting that $\Delta(\Delta G^\circ_{rc})_{NMF-H_2O}$ for Co(EMFMEoxosar-H)$^{2+/+}$ is somewhat larger at the electrode surface than in solution. A detailed examination of transfer free energies between a variety of solvents [4b] for Co(EFMEoxosar-H)$^{2+/+}$ in solution indicates that the values are influenced by solvent–acceptor interactions with the electron-rich enolate group. Since water is a better electron acceptor than NMF [17] electron-pair donation from a ligand to the solvent will lead to less positive values of $\Delta(\Delta G^\circ_{rc})_{NMF-H_2O}$. With adsorbed Co(EFMEoxosar-H)$^{2+/+}$ electron-pair donation to the solvent cannot occur if, as suggested above, the oxygens are bound to the mercury surface. This mode of surface coordination can therefore account for the larger values of $\Delta(\Delta G^\circ_{rc})_{NMF-H_2O}$.

These results demonstrate that substantial differences in the redox thermodynamics of surface-bound and bulk-phase redox couplex can arise which are attributable to the influence of the electrode surface upon the reactant–solvent interactions.

TABLE 2

Free energies of transfer, $\Delta(\Delta G_{rc}^{\circ})_{NMF-H_2O}$ [a], of Co(III)/(II) redox couples in bulk and surface-bound environments from water to N-methylformamide

Redox couple	Environment	$\Delta(\Delta G_{rc}^{\circ})_{NMF-H_2O}$/kJ mol^{-1} [a]
Co(EFMEoxosar-H)$^{2+/+}$ [b]	bulk	17.0 [c]
Co(EFMEoxosar-H)$^{2+/+}$ [b]	mercury surface	30.5
Co(diNOsar)$^{3+/2+}$ [b]	bulk	20.4 [c]
Co(sepulchrate)$^{3+/2+}$ [d]	bulk	26.5 [e]
Co(en)$_3^{3+/2+}$ [f]	bulk	23.5 [e]

[a] Values of $\Delta(\Delta G_{rc}^{\circ})_{NMF-H_2O}$ determined from measured formal potentials in H_2O and NMF, using TATB assumption as outlined in ref. 6b.
[b] For structures, see Fig. 1.
[c] Determined from data in Table 1.
[d] Sepulchrate = 1,3,5,8,10,13,16,19-octaazabicyclo[6.6.6]icosane.
[e] From data in ref. 6b.
[f] en = ethylenediamine.

The identification of such effects is greatly facilitated by separating the formal potential shifts into entropic and enthalpic components. Systematic studies along these lines for simple one-electron redox couples should not only provide valuable information on the nature of ionic solvation at electrode surfaces but may also shed light on the influence of the interfacial environment on the kinetics of heterogeneous electron transfer.

ACKNOWLEDGEMENTS

P.A.L. gratefully acknowledges support from a CSIRO fellowship. The research program of M.J.W. was supported in part by the Air Force of Scientific Research and the Office of Naval Research.

REFERENCES

1 For reviews, see R.W. Murray, Acc. Chem. Res., 13 (1980) 135; K.D. Snell and A.G. Keenan, Chem. Soc. Rev., 8 (1979) 259; W.R. Heineman and P.T. Kissinger, Anal. Chem., 52 (1980) 138R; M.D. Ryan and G.S. Wilson, Anal. Chem., 54 (1982) 20R.
2 J.T. Hupp and M.J. Weaver, J. Electroanal. Chem., 143 (1983) 43.
3 A.M. Sargeson, Chem. Brit., 15 (1979) 23.
4 (a) A.M. Bond, G.A. Lawrence, P.A. Lay and A.M. Sargeson, Inorg. Chem., 22 (1983) 2010; I.I. Creaser, A.M. Sargeson and A.W. Zanella, Inorg. Chem., in press; (b) P.A. Lay, J.T. Hupp, A.M. Sargeson and M.J. Weaver, in preparation.
5 R.J. Geue, J. Mac B. Harrowfield, T.W. Hambley, A.M. Sargeson and M.R. Snow, J. Am. Chem. Soc., submitted; W. Petri, A.M. Sargeson and M.R. Snow, to be published; P.A. Lay, unpublished results.
6 (a) E.L. Yee, R.J. Cave, K.L. Guyer, P.D. Tyma and M.J. Weaver, J. Am. Chem. Soc., 101 (1979) 1131; (b) S. Sahami and M.J. Weaver, J. Electroanal. Chem., 122 (1981) 155, 171.
7 E. Laviron, J. Electroanal. Chem., 100 (1979) 263.

8 H. Angerstein-Kozlowska and B.E. Conway, J. Electroanal. Chem., 95 (1979) 1; E. Laviron, J. Electroanal. Chem., 97 (1979) 135.
9 W. Petri and A.M. Sargeson, unpublished results.
10 For example, see H.B. Herman, R.L. McNeely, P. Surana, C.M. Elliott and R.W. Murray, Anal. Chem., 46 (1974) 1258.
11 L.M. Baugh and R. Parsons, J. Electroanal. Chem., 40 (1972) 407.
12 P. Daum and R.W. Murray, J. Electroanal. Chem., 103 (1979) 289.
13 E. Laviron and L. Roullier, J. Electroanal. Chem., 115 (1980) 65.
14 E.L. Yee and M.J. Weaver, Inorg. Chem., 19 (1980) 1077.
15 S. Sahami and M.J. Weaver, J. Solution Chem., 10 (1981) 199.
16 J.T. Hupp and M.J. Weaver, J. Electrochem. Soc., in press.
17 V. Gutmann, The Donor-Acceptor Approach to Molecular Interactions, Plenum Press, New York, 1978, Ch. 2.